CYCLIC AMP AND THE INDUCTION OF REACTIVE ASTROGLIOSIS

THESIS

Presented to the Graduate Council
of Texas State University-San Marcos
in Partial Fulfillment
of the Requirements

for the Degree

Master of SCIENCE

by

Mayuri P. Patel, B. A.

San Marcos, Texas
May 2010

CYLIC AMP AND THE INDUCTION OF REACTIVE ASTROGLIOSIS

Committee Members Approved:

_____

Joseph R. Koke, Thesis Chair

_____

Dana M. García

_____

Timothy Raabe

_____

Jeffrey Gross

Approved:

_____

J. Michael Willoughby
Dean of the Graduate College

COPYRIGHT

by

Mayuri Pankaj Patel

2010

ACKNOWLEDGEMENTS

I would like to express my gratitude to Dr. Joseph Koke, who always had his door open for my many questions and mistakes. I would like to thank my committee members, Drs. Dana García, Timothy Raabe, and Jeffrey Gross, for being a part of my committee. This thesis would not have been possible without my advisor and committee members' advice and guidance. I would also like to thank Dr. Weckerly on advice about statistical analyses. I would like to thank Dr. Shannon Weigum for sharing her extensive knowledge about cell culturing.

I would like to thank my amazing lab mates and friends who were always there for a much needed break. I am forever indebted to Katherine Saul and Elizabeth Capalbo who were always there to teach me new techniques and discuss "real science." To Gina Soto, I am so blessed to have you as a friend, you were always there to pick me up when I was down. To Luis, thank you for always being around for a break. To Marilyn Lim, thank you for being such a good listener and only being a phone call away.

Last but not least, I also thank my family, Mom, Dad, Mihir, Dada, and my late grandmother for always being there for me and encouraging me to keep going when I believed I wasn't able to continue. Everything I do is for my family. This thesis would definitely not have been possible without your support.

This manuscript was submitted on November 3, 2009.

TABLE OF CONTENTS

Page

LIST OF TABLES

LIST OF FIGURES

ABSTRACT

CYCLIC AMP AND THE INDUCTION OF REACTIVE ASTROGLIOSIS

by

Mayuri Pankaj Patel, B.A.

Texas State University-San Marcos

May 2010

SUPERVISING PROFESSOR: JOSEPH KOKE

Astrocytes play a major role in nerve regeneration of the central nervous system. In response to central nervous system (CNS) trauma or pathology such as neurodegeneration or ischemia, astrocytes react by exhibiting hypertrophy of their cellular processes and hyperplasia (proliferation), a process referred to as reactive astrocytosis. Reactive astrogliosis can be modeled *in vitro* using mechanical (scratch wound) or chemical stimuli to activate F98 rat glioblastoma cells from a quiescent state to a reactive-like state. Studies have shown monoclonal antibody (mAB) J1-31 may recognize a phosphoepitope found on the nuclear intermediate filament, lamin, as well as

the cytoplasmic intermediate filament characteristic to mammalian astrocytes, glial fibrillary acidic protein (GFAP), suggesting that mAB J1-31 is an appropriate marker for astrocytes entering the reactive state.

Reactive astrogliosis, as detected by increased labeling of cytoplasmic and nuclear epitopes by mAB J1-31, can be modeled *in vitro* by treatment of F98 cells with forskolin, an activator of adenylyl cyclase. Here I tested the hypothesis that a cAMP-mediated intracellular pathway is involved in eliciting forskolin-induced reactivity in F98 cells, and I attempted to elucidate that pathway using inhibitors of known cAMP-dependent downstream signaling molecules and fluorescent Ca^{+2} indicators and characteristic nuclear labeling of F98 cells by mAB J1-31. Forskolin was found to significantly increase labeling with mAB J1-31 in as little as 7 minutes, reaching a maximum after 30 minutes. Pretreatment of F98 cells with the protein kinase A (PKA) inhibitor H89 abolished the effect of forskolin, while inhibitors of protein synthesis and L-type calcium channels had no effect. Forskolin was found to induce transient cytoplasmic increases in Ca^{+2} levels (as measured by Oregon Green conjugated BAPTA), and the relation of this to PKA is currently under investigation. On the basis of these results, it appears that induction of cAMP production in F98 cells results in a PKA-dependent increase in phosphorylation of cytoplasmic and nuclear intermediate filaments, which may indicate the first stages of F98 cell transition from normal to a reactive state.

CHAPTER I

INTRODUCTION

The brain is composed of two major cell types: neurons and glia (Svendsen, 2002). Glial cells outnumber neurons 10:1 although neurons have long been considered the key players in the nervous system (Temburni and Jacob, 2001). Glia comprise four types of cells: oligodendrocytes, Schwann cells, microglia, and astrocytes. Glial cells were once thought to play a supportive role holding neurons in place; however, each glial cell has now been characterized to have a specialized function (Agulhon et al., 2008). Here I focus on astrocytes and the cell signaling pathway leading to reactive astrogliosis.

Astrocytes, the most abundant glial cell, have multiple functions in the central nervous system (CNS), including maintaining homeostasis, releasing and taking up neurotransmitters, and stabilizing neuronal synapses (Chen and Swanson, 2003). Astrocytes express various neurotransmitter receptors and ion channels, which enable them to respond to neuronal activity via calcium waves (Braet et al., 2004; Schemes and Giaume, 2006).

Astrocytes also play a major role in forming a barrier to nerve regeneration of the central nervous system. In response to any central nervous system (CNS) trauma such as neurodegeneration or ischemia, astrocytes react by exhibiting hypertrophy of their cellular processes and proliferation, a reaction often referred to as reactive astrogliosis

(Eng and Ghirnikar, 1994; Pekny and Pekna, 2004; García and Koke, 2009). Reactive astrogliosis is characterized by an upregulation or reorganization of the intermediate filaments glial fibrillary acidic protein (GFAP), nestin and vimentin (Pekny and Nilsson, 2005) and also phosphorylation of lamin B (García et al., 2003). In this way, the astrocytes form a glial scar that prevents further damage to healthy tissues but may also produce pathological effects that interfere with residual neuronal circuits, prevent remyelination or form a physical barrier impeding axonal regeneration (Malhotra et al., 1990; Silver and Miller, 2004). It is therefore important to identify the intracellular molecular mechanisms involved in the activation of astrocytes.

The extracellular signaling pathways causing astrocytes to become reactive are many; for a review, see Malhotra et al. (1990) or Correa-Cerro and Mandell (2007). Intracellular signaling pathways triggering astrocytes to leave the quiescent state and reactivate the cell cycle, leading to hypertrophy and hyperplasia, are much less well characterized. These pathways are likely overlapping and redundant and may vary according to the external signal evoking the response. For example, Jagged1, a ligand for the Notch signaling pathway, is upregulated when cultured astrocytes are exposed to lipopolysaccharide (LPS). Jagged1 inhibition by siRNA has anti-inflammatory effects in astrocytes shown by a decrease of proinflammatory cytokines (IL1β, IL1α, and TNFα), suggesting that the Notch signaling pathway regulates inflammation in the CNS through possible crosstalk with NFκB and JAK/STAT/SOCS pathways (Morga et al., 2009). Kohyama et al. (2008) has shown the JAK/STAT pathway to induce differentiation of oligodendrocytes into GFAP-positive cells. GFAP expression in oligodendrocytes was observed *in vitro* when the oligodendrocytes were stimulated by leukemia inhibitory

factor (LIF), an astrocyte-inducing cytokine.   In vivo studies indicate that oligodendrocytes transition to GFAP-positive astrocytes in lesioned rat but not in unlesioned rats, indicating that oligodendrocytes to astrocytes transition occurs via the JAK/STAT pathway after injury (Kohyama et al., 2008). Reports indicate that cross-talk between PKA/CREB and JAK/STAT pathways occur in cells other than astrocytes, such as osteoblasts. Murrills et al. (2009) investigated non-cyclic AMP pathways resulting in CREB phosphorylation using Saos-2 human osteosarcoma cells that were transfected with CRE linked to a luciferase reporter. They used epidermal growth factor (EGF) which activates multiple pathways including JAK/STAT in a non-cAMP induced manner, and found that EGF has little effect on CRE when used alone; however, in combination with parathyroid hormone (PTH), EGF induced a synergistic and dose-dependent stimulation of CRE-Luciferase activity (Murrills et al., 2009). Cross-talk among signaling pathways leading to cAMP response element (CRE) activation or repression seems likely given the large size of the cAMP response element binding protein (CREB) family and the wide range of possible hetero- and homodimerizations.

The involvement of CREBs in transitioning astrocytes to the reactive state raises the possibility that intracellular production of cAMP by activation of adenylyl cyclase may be an initial step in conversion of quiescent to reactive astrocytes. Cyclic-AMP is produced by the conversion of ATP into cAMP by adenylyl cyclase, usually under the influence of G-protein coupled receptors.   However, other activators of adenylyl cyclase may exist in astrocytes. Hydrogen sulfide (H_2S) has been shown to act as a cell to cell signal in the CNS, and its target in astrocytes appears to be adenylyl cyclase (Nagai et al., 2004). Elevation in cAMP seems to activate cAMP-gated Ca^{+2} channels leading to an

increase in intracellular calcium levels. The rapid rise in cytoplasmic Ca^{+2} may propagate from cell to cell via gap junctions as the well characterized calcium "waves" that can be visualized both in situ and in vitro in primary cultures of astrocytes (Qu et al., 2008).

Cyclic AMP has multiple downstream targets, of which the best characterized is protein kinase A (PKA). Inactive PKA is a tetrameric structure consisting of two catalytic subunits and two regulatory subunits. Cyclic AMP binds to the two regulatory subunits causing the dissociation of the catalytic subunits. The liberated catalytic subunits phosphorylate downstream target protein phospho-motifs containing serine or threonine, in the cytoplasm or in the nucleus (Kim et al., 2005; Kamenetsky et al., 2006; see Figure 1).
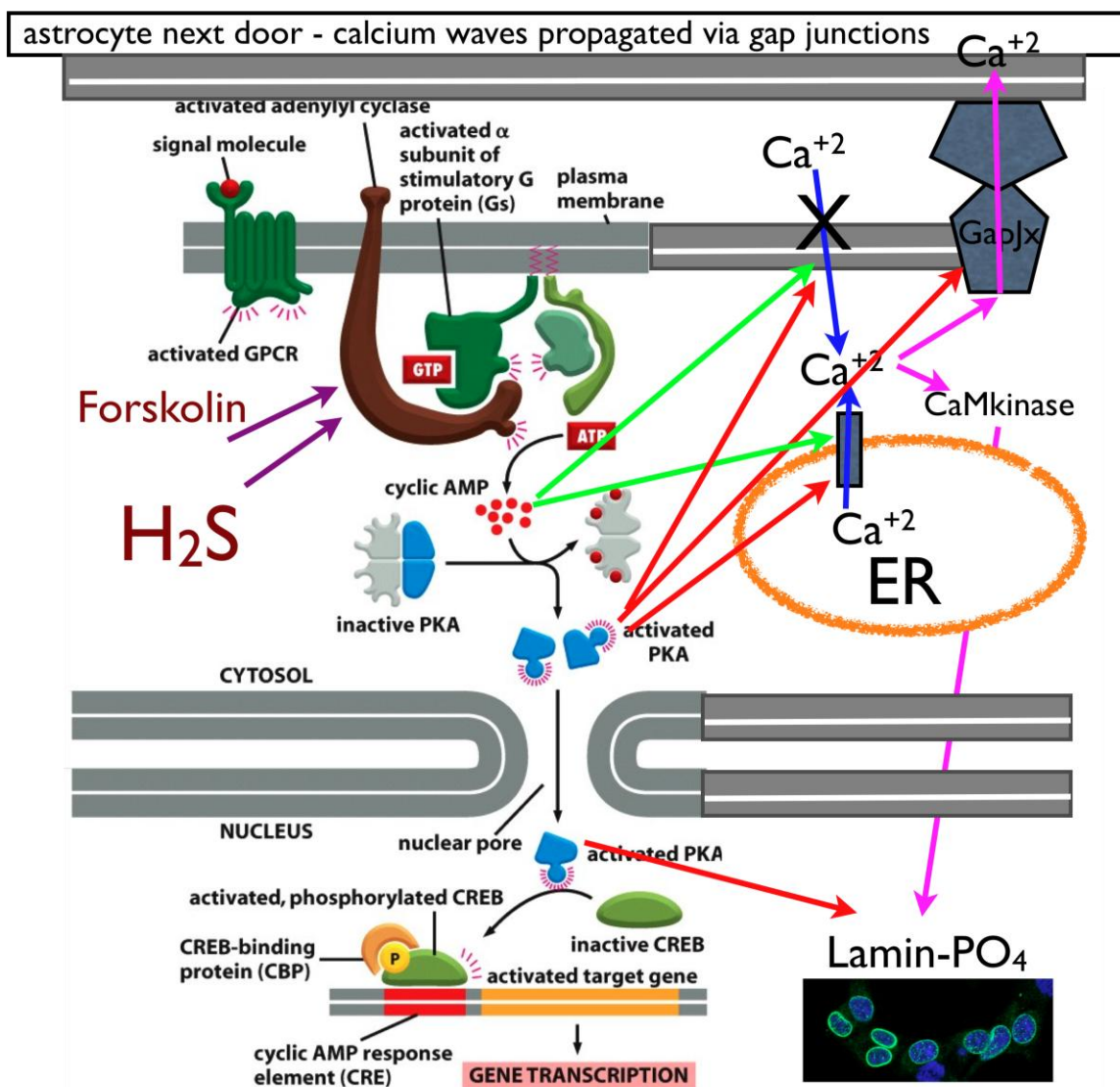
Figure 1. Diagrammatic representation of possible signaling pathway involving cAMP and reactive astrocytes. There are multiple pathways that may be implicated in forskolin-induced reactivity. Forskolin activates adenylyl cyclase which catalyzes the conversion of ATP to cAMP. Cyclic AMP then binds to the regulatory subunits of PKA and liberates the catalytic subuntis of PKA to affect downstream targets. I have found that inhibiting the catalytic subunits of PKA using H89 yields a decrease in mAB J1-31 labeling indicating a PKA mediated pathway may be involved in forskolin-induced reactivity. Other possible pathways need to be investigated further. Cyclic-AMP may open cAMP-gated $Ca+2$ channels located on the plasma membrane or located on the endoplasmic reticulum. Activated PKA may also open these calcium channels or have an affect on gap junctions or phosphorylate lamins through CaM kinase mechanisms. Finally, another mechanism may involve activated PKA/CREB pathways phosphorylating nuclear lamins. Modified from Figure 15-41a, *Molecular Biology of the Cell*. (c) 2008 From (or Adapted from) Molecular Biology of the Cell 5E by Alberts et al. Reproduced by permission of Garland Science/Taylor and Francis LLC.

Reactive astrogliosis has been modeled in vitro using primary cultures, C6 cells and rat glioma F98 (a.k.a. 9L) cells grown on coverslips (Yang et al., 2009) and subjected to chemical or mechanical stimulation ("scratch-wound," Malhotra et al., 1997). Astroglial cells in scratched monolayers exhibit the hallmarks of reactive astrogliosis of F98 cells, i.e., cell hypertrophy and increased immunostaining for GFAP and a shift in cell morphology from a flat, polygonal shape into a stellate, compact cell with numerous thin cytoplasmic processes (Won and Oh, 2000).

Cyclic AMP has been shown to have important roles in astrocytes. The addition of cAMP to primary astrocyte cultures, which are normally not stellate, leads to astrocyte stellation (Won and Oh, 2000), a characteristic of reactive astrocytes. Ramsey et al. (2005) used forskolin (an activator of adenylyl cyclase) and dibutyryl cAMP (dbcAMP, a membrane permeant cAMP derivative resistant to phosphodiesterase) and found both effective in induction of the reactive state in F98 glioblastoma cells. Elevation of cAMP by dbcAMP has also been shown to induce a reactive state in primary cultures of C6 cells, a rat glioblastoma similar to the F98 cell line. They observed astrocyte differentiation and measured reactivity by showing an increase in catalase activity (Makino et al., 2008).

Immunocytochemistry identifies reactive astrocytes by increases in expression of GFAP protein, the accepted marker for reactive astrocytes (Silver and Miller, 2004). In 1984, Malhotra et al. raised mAB J1-31 against human brain homogenates from multiple sclerosis (MS) plaques. García et al. (2003), on the basis of strong circumstantial evidence, speculated that mAB J1-31 binds to a phosphorylated epitope on GFAP and

nuclear lamins. The putative phosphorylation amino acid sequences of GFAP and lamin B contain a single serine (Ser-68) residue that was located in a PKA consensus sequence (García et al., 2003). These observations led Ramsey et al. (2005) to test if elevating cAMP levels in F98 cells, either by the activation of adenylyl cyclase using forskolin or by addition of dbcAMP would result in increased mAB J1-31 labeling, which it did. Ramsey et al. (2005) further verified that mAB J1-31 labeled cytoplasmic filaments also labeled by anti-GFAP and nuclear rings and "dots" also labeled by anti-lamin B, and that forskolin treatment of F98 cells did not increase the labeling intensity of anti-GFAP or anti-lamin B. However, some of the results obtained by Ramsey et al. conflict with the present study, particularly regarding the effect of PKA inhibition by H89.

Here, I test the hypothesis that a cAMP-mediated intracellular pathway is involved in eliciting forskolin-induced activation of F98 cells, as a proxy for reactive astrocytes. Using mAB J1-31 as an indicator, I attempt to better understand the cAMP pathway in activation of astrocytes. As shown by Ramsey et al. (2005), treatment of F98 cells in vitro with forskolin can activate cells as measured by staining with mAB J1-31. I treated ~90% confluent F98 glioma cultures with forskolin for to analyze the time course of the forskolin effect.   This study revealed that forskolin induced the F98 cells to become reactive, as measured by a statistically significant increase in mAB J1-31 binding, as early as 7 minutes after addition of forskolin, reaching a maximum at 30 minutes.

To further explore the effects of elevated cAMP in this model, I addressed three questions: Is forskolin-induced activation of F98 cells PKA-dependent, protein synthesis dependent, or dependent on L-type or other calcium channels? I also investigated the

specificity of mAB J1-31 for phosphoepitopes further by phosphatase treatment of F98 cell extracts followed by SDS-PAGE and western blot analysis.

CHAPTER II

MATERIALS AND METHODS

Cell Culture

F98 rat glioblastoma (ATCC, #CRL-2397, Manassas, VA) and J1-31 hybridoma (ATCC, #CRL-2253, Manassas, VA) cells were obtained from the American Type Culture Collection and were seeded from frozen stock cultures in fetal bovine serum (FBS, Sigma, St. Louis, MO) with 10% dimethyl sulfoxide (DMSO, Sigma, St. Louis, MO) stored in liquid nitrogen. Cells were rapidly thawed and DMSO was removed by centrifugation at 2500 rpm followed by resuspension of the cell pellet in minimum essential medium (MEM, Sigma, St. Louis, MO) containing 10% FBS, 2 mM L-glutamine and 10,000 U penicillin and10,000 mg/ml streptomycin. The cell density was determined using a hemacytometer (Fisher Scientific, Pittsburg, PA) and diluted appropriately to maintain an initial seeding density of 4.0×10^4 cells/cm^2 of surface area. Cell cultures were seeded into 25 cm^2 culture flasks with 5 ml MEM or 150 cm^2 culture flasks with 15 ml MEM and maintained at 37°C in a humidified atmosphere containing 5% CO_2 for 24-96 hours. Cells cultured on glass coverslips were also seeded from frozen stock cultures, and plated into 40 mm x 11 mm or 150 mm x 20 mm petri dishes containing (22 mm x 22 mm) glass coverslips and 2 ml or 20 ml of MEM, respectively. The cells were allowed to grow in culture for 24-96 hours.

Forskolin Time Course

Cells were grown to approximately 90% confluency. Each experiment was done on the same batch of cells at the same stage of growth. It is important for all the cells to be at the same stage of growth because García et al. (2003) showed a relationship between time in culture and mAB J1-31 labeling of nuclei.

The time-course of the forskolin effect on mAB J1-31 labeling was determined by adding 4 μM forskolin (prepared from a stock solution of such and such concentration dissolved in DMSO) to cultures of F98 cells grown on coverslips, and then withdrawing the coverslips at these intervals: 1, 3, 5, 7, 15, 30, 45, 60, 75, 90, 105, and 120 minutes. After withdrawing the coverslips from the treatment each coverslip was fixed in ice-cold methanol, and immunostaining using mAB J1-31 followed by an Alexa-fluor 488-conjugated (Invitrogen, Eugene, OR) secondary antibody. Staining intensity was measured using Olympus FV10-ASW ver.01.07 (Olympus Corporation, Tokyo, Japan) by outlining individual cells (N=10) and calculating mean pixel intensity/unit area (μm^2). I analyzed the data, with or without log transformation as appropriate to satisfy the assumption of homoscedasticity. The data were exported to an Excel spreadsheet, and StatPlus (Analystsoft statistical package for Mac - www.analystsoft.com/en/products/statplus/) was used to calculate means, standard errors, and perform the ANOVA with significance determined from the Tukey's HSD post-hoc tests.

Experimental Treatments

All materials and reagents were supplied by Sigma St. Louis, MO, unless otherwise specified. All treatment reagents were dissolved in 3 ml fresh culture medium

at the concentration indicated in Table 1. Cells were exposed to the reagents by replacing

3 ml of culture medium with 3 ml of the experimental treatment medium. Reagents listed

in Table 1 include forskolin, an adenylyl cyclase activator; cycloheximide, a protein

synthesis inhibitor; H89, a selective inhibitor of PKA catalytic subunits; Rp-cAMPS, a

selective inhibitor of PKA regulatory subunits; puromycin, a protein synthesis inhibitor;

and verapamil, a Ca^{2+} L-type channel inhibitor. Each experimental treatment lasted 10

minutes followed by a 20-minute forskolin treatment. Forskolin was applied into the

culture medium that contained the inhibitor, as indicated in Table 1.

Table 1. Treatment reagents, dilutions, solvent, and literature references. All reagents in
the table were supplied by BIOMOL International, Plymouth Meeting, PA.

Agent	Final Concentration	Solvent	Literature Reference
Forskolin	4 µM	DMSO	Seamon et al., 1981
*Cycloheximide	10 µM	DMSO	Obrig et al., 1970
Puromycin	10 µM	H_2O	Nathans, 1964
H89	48 nM	DMSO	Chijiwa et al., 1990
Rp-cAMPS	100 µM	H_2O	Gjertsen et al., 1995
Verapamil	2 µM	H_2O	Agrawal et al., 2000

*Cycloheximide treatments were examined and concluded to not be representative of
actual results due to the detachment of most of the F98 cells during treatment. Therefore
the results from this treatment group are not reported.

At the end of the treatment period, coverslips bearing cells were removed, washed

in phosphate buffered saline (PBS; 137mM NaCl, 2.7 mM KCl, 4.3 mM Na_2HPO_4, 1.4

mM KH_2PO_4, pH 7.4) in order to remove all residual medium remaining on the culture

surface, then fixed by immersion in ice cold methanol (-20˚C) for 1 minute. After

fixation, cells on coverslips were allowed to air dry and were stored at -20˚C, then

rehydrated in PBST at room temperature prior to immunostaining.

Immunohistochemistry

Coverslips bearing cells were treated with 20% non-fat powdered milk in PBS for 2 hours at room temperature to block non-specific binding sites. The coverslips were then washed three times in PBS containing 0.2% Tween-20 (PBST) over a period of 30 minutes.

Coverslips were incubated overnight at 4˚C in mAB J1-31 (see Table 2), washed three times in PBS, then incubated in secondary antibody at room temperature for 2 hours. Appropriate secondary antibody was diluted as recommended by their suppliers (Table 3). After incubation in secondary antibody, the coverslips were incubated in DAPI for 5 minutes and again washed three times in PBS, then mounted using 90% glycerol in PBS. Immunostaining negative controls were performed by replacing the primary antibody with PBS.

Table 2. Primary antibodies and dilutions used for immunofluorescence (mAB J1-31) and western blot analysis (all).

Antibody (Catalog #) Specificity	Species/Isotype	Dilution for fluorescence and western blot analysis	Source
J1-31 mAB from hybridoma cell line (CRL-2253)	Mouse IgG	Undiluted culture supernatant	American Type Culture Collection, Rockville, MD
Anti-GFAP pAB (G9269)	Rabbit IgG	1:400 in PBS	Sigma Chem. Co., St. Louis, MO
Anti-phosphoserine mAB (P3430)	Mouse IgG1	1:1000 in PBS	Sigma Chem. Co., St. Louis, MO
Anti-laminin B2 (33-2100)	Mouse IgG1-kappa	1:200 in PBS	Invitrogen, Eugene, OR

Image Acquisition

Images were acquired using the Olympus FV1000 confocal microscope. All images collected for qualitative and quantitative analysis were done so at an optical magnification of 60X. Gain and dynamic range settings were calibrated on forskolin treated cells, and then kept unchanged for recording of the experimental control and inhibitor treated cells, thus allowing quantitative comparisons to be made. Final production of images for publishing was done on an Apple Macintosh G5 (Cupertino, CA) running Adobe Photoshop CS3 (San Jose, CA). Images shown in Results are examples. Each of the experiments in which the outcome was determined by immunofluorescence labeling was performed in triplicate.

Quantification of Staining Intensity

Staining intensity was measured using Olympus Fluoview software by outlining individual cells (n=10) and calculating mean pixel intensity/unit area (μm^2). I analyzed the data, with or without log transformation as appropriate to satisfy the assumption of homoscedasticity. The data were exported to an Excel spreadsheet, and StatPlus (Analystsoft statistical package for Mac - www.analystsoft.com/en/products/statplus/) was used to calculate means, standard errors, and perform the ANOVA with significance determined from the Tukey's HSD post-hoc tests.

BAPTA Cell Loading

F98 cells cultured on coverslips were loaded with Oregon Green 488 BAPTA-1 dextran (O6798, Invitrogen, Carlsbad, CA) by placing coverslips bearing cells on a pedestal and incubating in 100 µl of hypertonic loading medium at 37° for 10 minutes according to the manufacturer's instructions.

Live cell imaging was conducted using the FV1000 confocal microscope. One-thousand frames were collected for each trial. The first 200 frames of each trial serve as controls by viewing only F98 cells loaded with Oregon Green 488 BAPTA-1. The next 800 frames served as experimental treatments after 4 μM forskolin was added to the dish containing the coverslip with F98 cells. Image acquisition was done in near real-time, collecting approximately 1 frame/sec for a total observation time of 17 minutes.

Preparation of Cell Lysates for Electrophoresis and Western Blot Analysis

F98 cells were seeded at an initial density of 4.0×10^4 cells/cm^2 and grown in 75 cm^2 flasks for 3 days. At the time of treatment 15 ml of culture medium was replaced with 15 ml of fresh medium or 15 ml of fresh medium containing forskolin. After 20 minutes, the MEM was removed and cells were detached from the substrate using 15 ml EDTA/trypsin solution and incubated at 37°C for 5-10 minutes. The detached cells were transferred to a centrifuge tube and spun at 2500 rpm for 5 minutes. The pellet was resuspended in 2 ml of PBS and spun at 2500 rpm for 5 minutes. Homogenization buffer (5 volumes of 0.02 mM leupeptin, 0.01 mg/ml aprotinin, 0.1 mg/ml PMSF) was added to the cells and incubated on ice for 30 minutes. The lysates were run through a 20 gauge needle and aliquots of lysates were stored at -20°C. Lysates from untreated and forskolin treated cells were used to generate samples treated with or without H89 and protein phosphatase 2A$_1$ (PP2A$_1$) (#SE-119, BIOMOL, Plymouth Meeting, PA) for 30 minutes. Following phosphatase treatment, cell lysates were combined (4 parts to 1 part) with 5X sample buffer (60 mM Tris-HCL, 25% glycerol, 2% SDS, 14.4 mM 2-mercaptoethanol, and 0.1% bromophenol blue).

SDS-PAGE was performed as previously described (García et al., 2003). In some cases, 8.0 M urea was added to the sample buffer and TBE-Urea gels (#161-1116 Bio-Rad, Hercules, CA) were used to promote solubilization of the intermediate filament proteins, specifically GFAP and lamins. See Tables 2, 3 for the antibodies used.

Table 3. Secondary antibodies and probes used for immunofluorescence and western blot analysis.

Antibody/Probe (Catalog #)	Conjugate	Dilution	Supplier
Goat anti-mouse IgG (A11001)	Alexa Fluor 488	1:200 in PBS	Invitrogen, Eugene, OR
Goat anti-mouse polyvalent (A0162)	Alkaline Phosphatase	1:4000 in PBS	Invitrogen, Eugene, OR
Goat anti-rabbit IgG (A3812)	Alkaline Phosphatase	1:30,000 in PBS	Sigma Chem. Co., St. Louis, MO

CHAPTER III

RESULTS

A. What is the time course of the forskolin effect on mAB J1-31 labeling?

In order to determine at the response time for maximal J1-31 labeling in response to forskolin, cells were fixed at various intervals after treatment. Forskolin was found to cause a statistically significant increase in labeling intensity within 7 minutes. The mean pixel intensity caused by mAB J1-31 labeling reached its peak at 30 minutes. After 30 minutes of exposure to forskolin, the intensity of mAB J1-31 labeling decreased with continued exposure to forskolin. A second increase in labeling was observed at 90 minutes. Since exposure of F98 cells to forskolin for 20-30 minutes showed the greatest mean pixel intensity/μm^2 among the time points examined, cells were exposed to forskolin for 20 minutes in subsequent experiments (Figure 2).
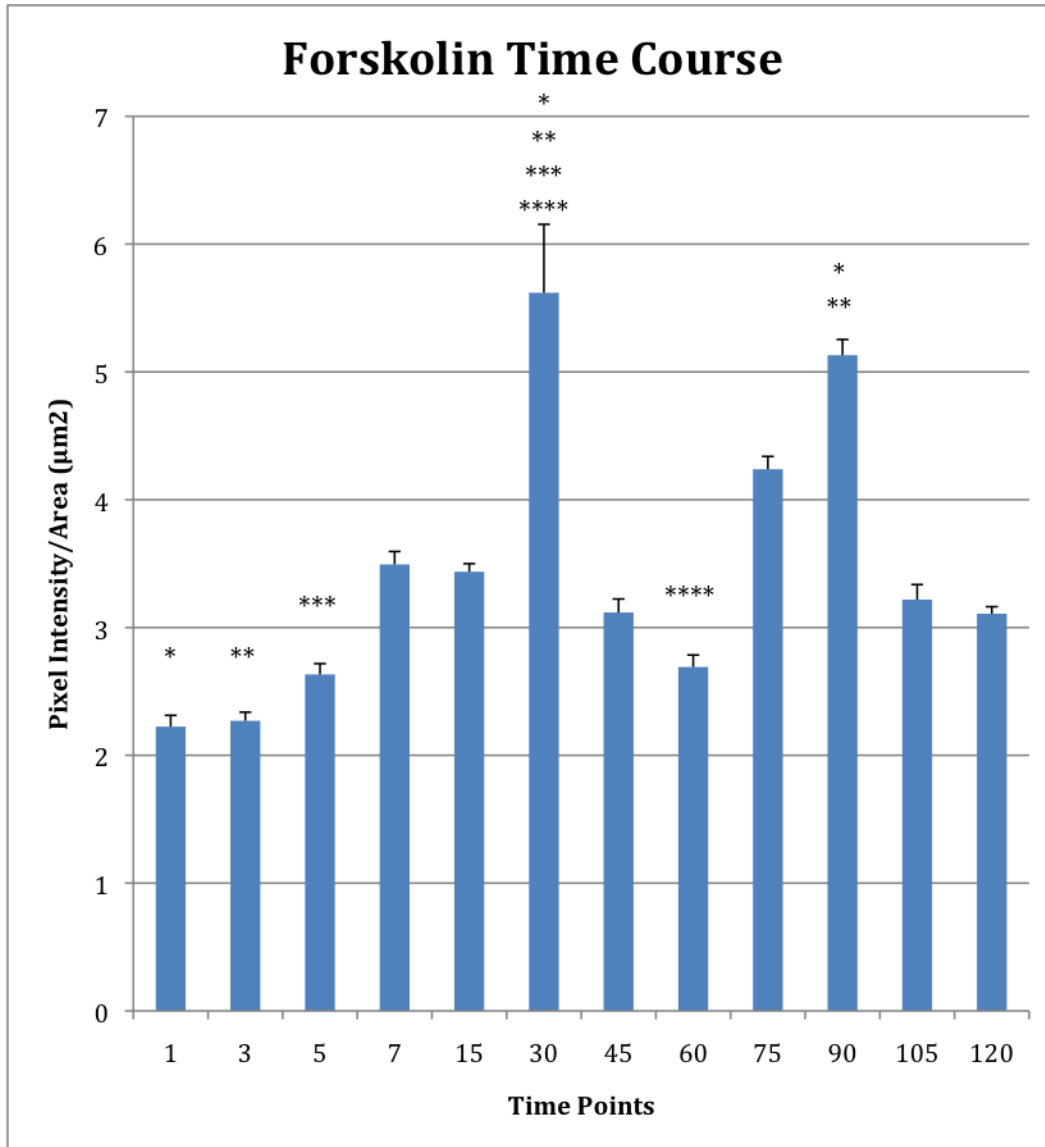
Figure 2. The effect of forskolin on mAB J1-31 labeling intensity as a function of time. N = 10 cells for each data point. Treatments in forskolin for 30 minutes and 90 minutes each are statistically different from 1 minutes and 3 minute treatments. The five minute treatment is also statistically significantly different from the 30 minute treatment. The 30 minute treatment is statistically different from the 60 minute treatment.

B. Is PKA involved in transitioning cells from a quiescent to reactive state, as measured by increased J1-31 labeling?

Immunostaining of nearly confluent F98 cells using mAB J1-31 revealed a nuclear lamin cortex and discrete dot-like objects within the nucleus of nearly confluent untreated F98 cells. To determine if forskolin-induced activation of F98 cells is PKA dependent, F98 cells were treated with two different PKA inhibitors: H89, which inhibits the catalytic site of PKA, and Rp-cAMPS which inhibits the regulatory site of PKA. H89 caused a reduction in mAB J1-31 labeling (Figure 3). This inhibition is visible in both F98 cells treated with H89 followed by forskolin treatment and F98 cells treated with H89 alone. Quantification of mAB J1-31 labeling revealed that treatment of F98 cells with H89 prior to treatment with forskolin resulted in a statistically significant decrease in mAB J1-31 labeling (Figure 8). However, quantification of mAB J1-31 labeling of F98 cells treated with Rp-cAMPS prior to treatment with forskolin (Figure 4) did not result in statistically significant decrease in comparison to F98 cells treated with forskolin alone (Figure 8).
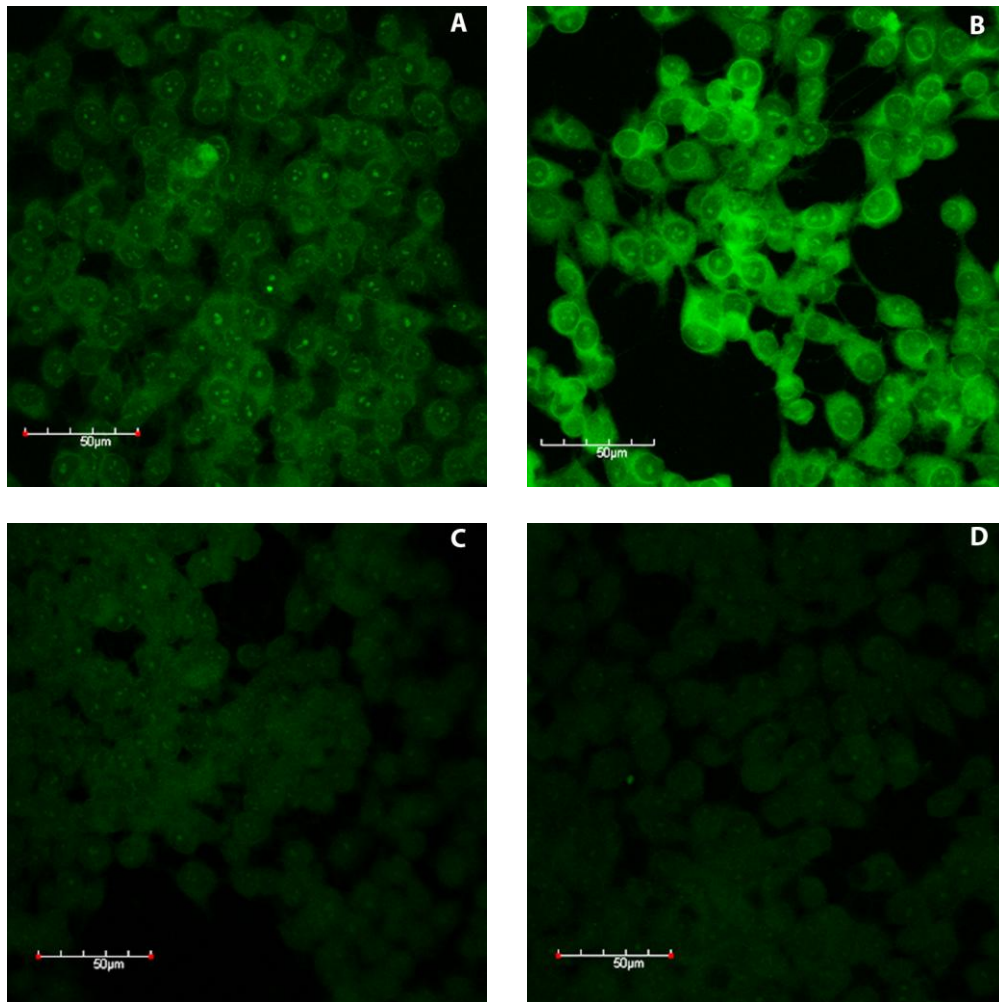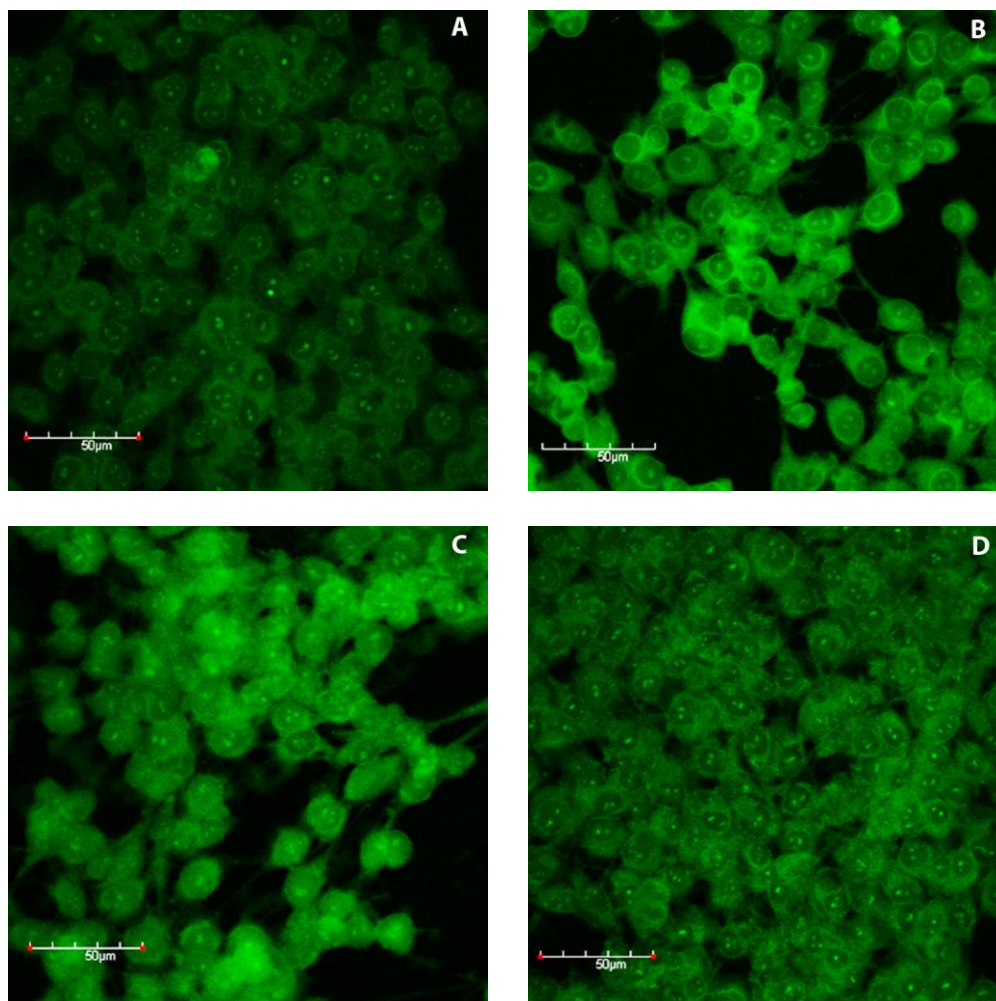
Figure 3. Confocal images of F98 cells treated to modulate PKA (H89). Cells were treated with H89 for 10 minutes followed by a 20 minute incubation in forskolin with subsequent fixation in methanol and processing for immunocytochemical analysis, as described in the text. All panels show F98 cells probed with mAB J1-31 and labeled with a secondary antibody conjugated to Alexa Fluor 488.

  A. No treatment
  B. Forskolin treatment
  C. H89 followed by forskolin treatment
  D. H89 treatment

Figure 4. Confocal images of F98 cells treated to modulate PKA (Rp-cAMPS). Cells were treated with Rp-cAMPS for 10 minutes followed by a 20 minute incubation in forskolin with subsequent fixation in methanol and processing for immunocytochemical analysis, as described in the text. All panels show F98 cells probed with mAB J1-31 and labeled with a secondary antibody conjugated to Alexa Fluor 488.

    A. No treatment
    B. Forskolin treatment
    C. Rp-cAMPS followed by forskolin treatment
    D. Rp-cAMPS treatment

To determine if the forskolin-induced increase in mAB J1-31 labeling is
dependent on protein synthesis, cells were treated with cycloheximide and puromycin as
described in Methods. The results indicate an increase in mAB J1-31 labeling. This
increase is visually seen in both F98 cells treated with cycloheximide or puromycin
followed by forskolin treatment, as well as F98 cells treated with cycloheximide or
puromycin only. Puromycin showed a statistically significant increase in mAB J1-31
labeling in comparison to the forskolin on treated F98 cells. (Figure 5-6).
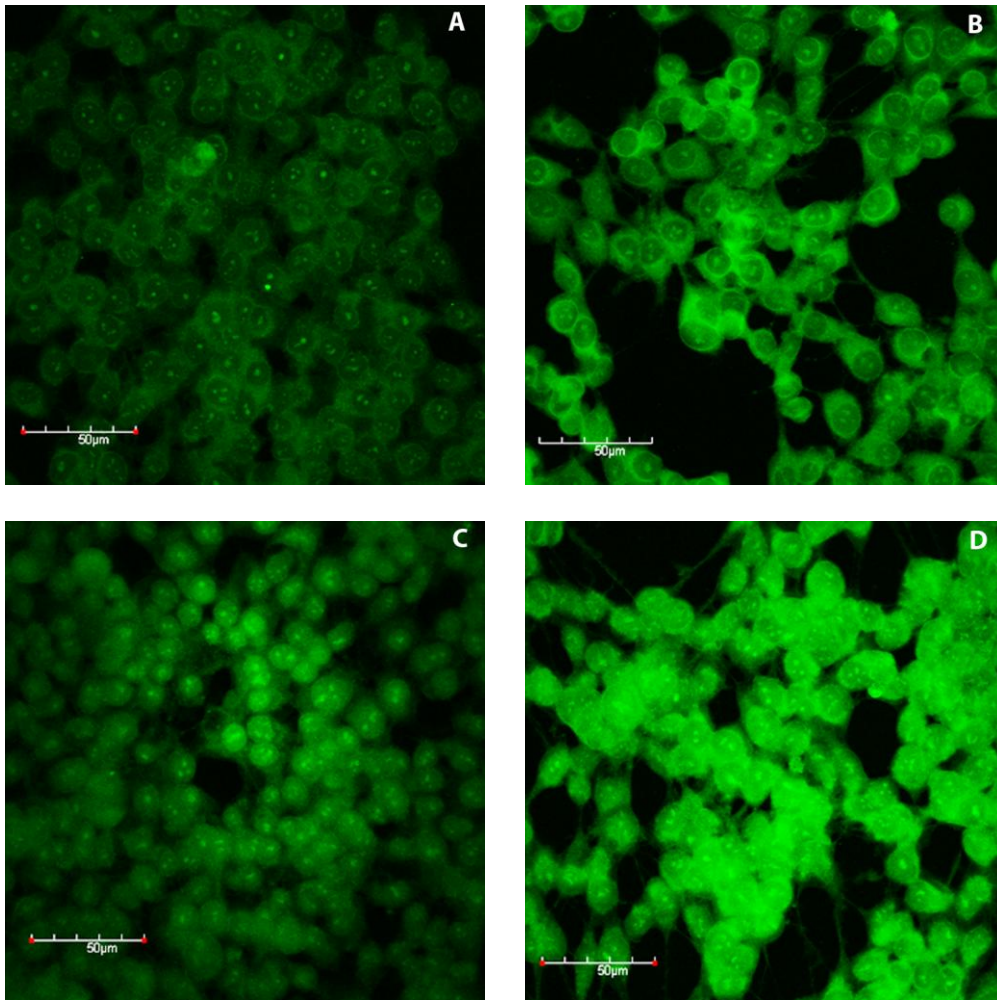
Figure 5. Confocal images of F98 cells treated to modulate protein synthesis (cycloheximide). Cells were treated with cycloheximide for 10 minutes followed by a 20 minute incubation in forskolin with subsequent fixation in methanol and processing for immunocytochemical analysis, as described in the text. All panels show F98 cells probed with mAB J1-31 and labeled with a secondary antibody conjugated to Alexa Fluor 488.

A. No treatment
B. Forskolin treatment
C. Cycloheximide followed by forskolin treatment
D. Cycloheximide treatment
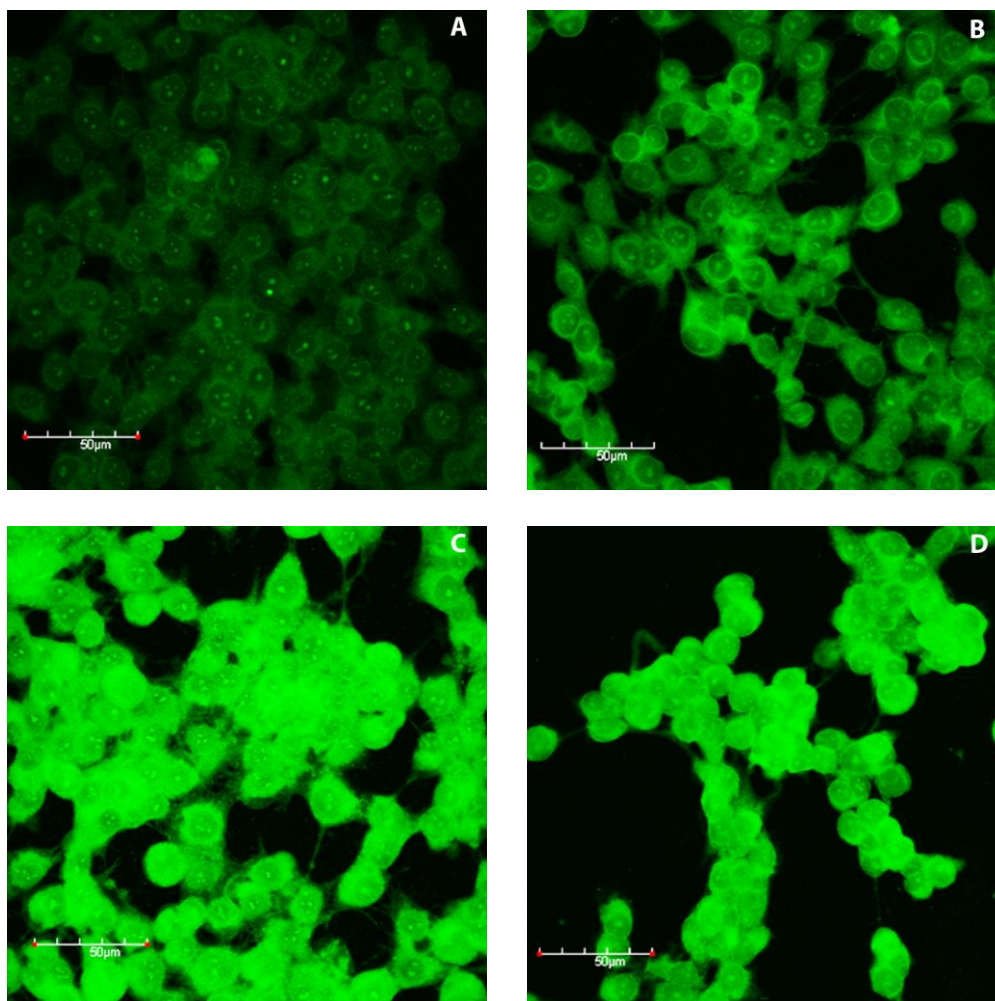
Figure 6. Confocal images of F98 cells treated to modulate protein synthesis (puromycin). Cells were treated with puromycin for 10 minutes followed by a 20 minute incubation in forskolin with subsequent fixation in methanol and processing for immunocytochemical analysis, as described in the text. All panels show F98 cells probed with mAB J1-31 and labeled with a secondary antibody conjugated to Alexa Fluor 488.

    A. No treatment
    B. Forskolin treatment
    C. Puromycin followed by forskolin treatment
    D. Puromycin treatment

To address the question on whether forskolin-induced activation of F98 cells is dependent on calcium influx from L-type calcium channels, the cells were treated with verapamil, an L-type calcium channel inhibitor. The results indicate an increase in mAB J1-31 labeling. This increase is seen in both F98 cells treated with verapamil followed by forskolin treatment as well as F98 cells treated with verapamil only. Quantification of mAB J1-31 labeling revealed that treatment of F98 cells with verapamil prior to treatment with forskolin resulted in a statistically significant increase in mAB J1-31 labeling when compared to cells treated with forskolin only (Figure 7).
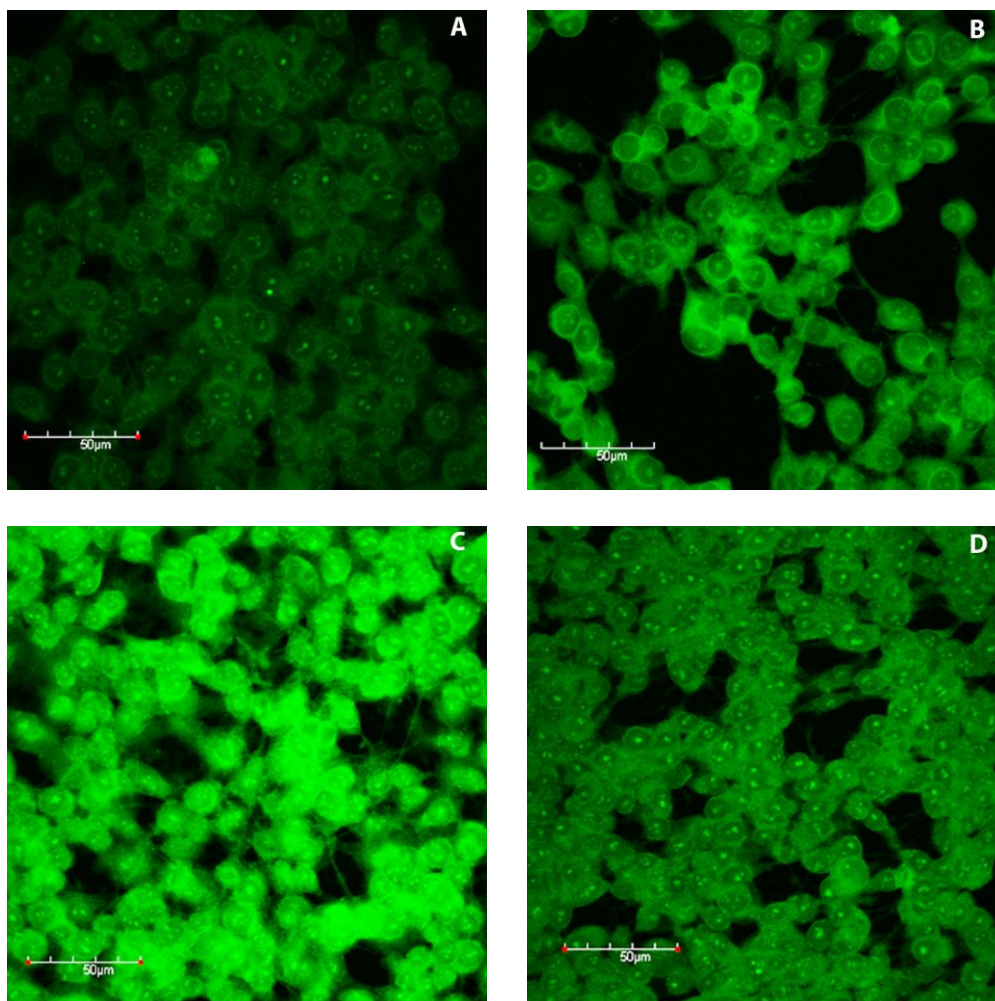
Figure 7. Confocal images of F98 cells. Cells were treated with verapamil for 10 minutes followed by a 20 minute incubation in forskolin with subsequent fixation in methanol and processing for immunocytochemical analysis, as described in the text. All panels show F98 cells probed with mAB J1-31 and labeled with a secondary antibody conjugated to Alexa Fluor 488.

A. No treatment
B. Forskolin treatment
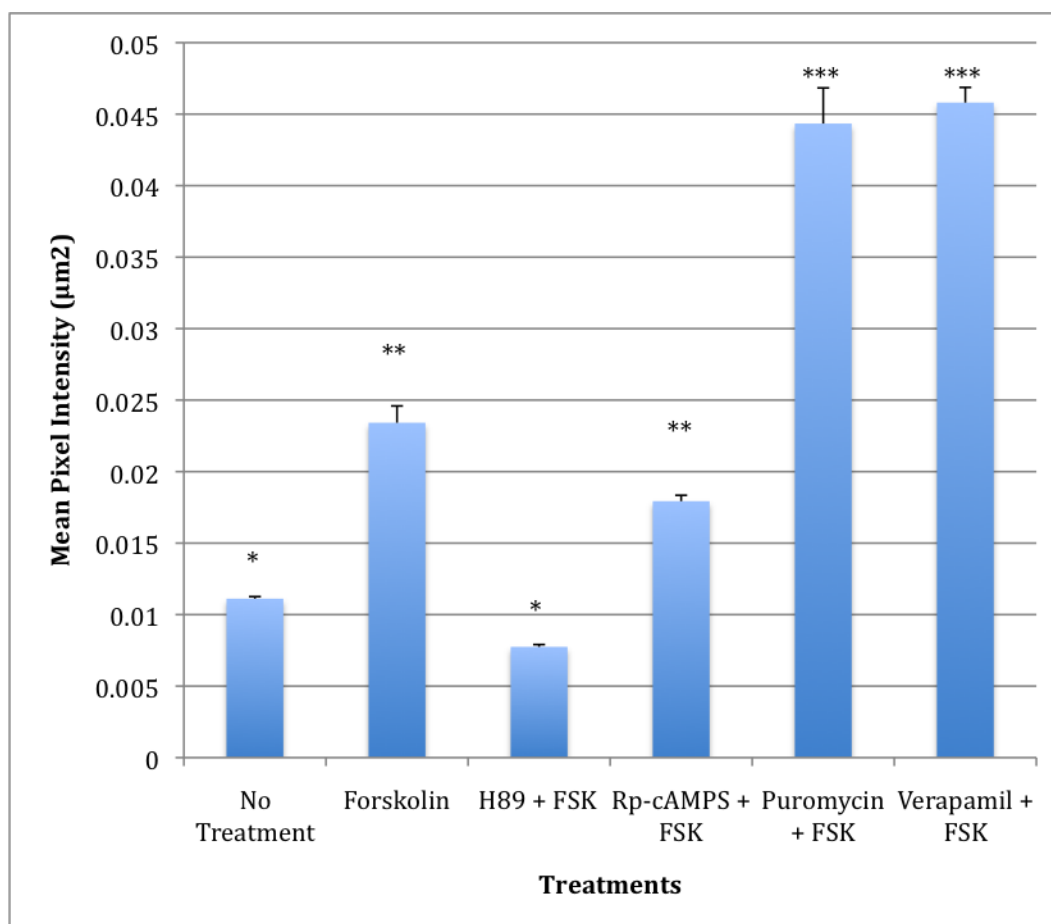C. Verapamil followed by forskolin treatment
D. Verapamil treatment

Figure 8. The effects of forskolin and various inhibitors on pixel intensity resulting from mAB J1-31 staining. N = 10 for each data column, and the error bars represent the standard errors of the mean.

C. Does forskolin cause opening of Ca^{+2} channels in F98 cells?

Previous research by Ramsey (2005) suggested that verapamil treatment reduced mAB J1-31 labeling in F98 cells. Therefore I tested for calcium transients in F98 cells in the presence and absence of forskolin. When live F98 cells loaded with Oregon Green 488 BAPTA-1 were viewed by confocal microscopy, minimal fluorescence was seen. Within 5 minutes of addition of forskolin, significant numbers of green flashes or "sparks" began to appear. These flashes were always cytoplasmic and most had durations of 5 to 15 seconds, although some persisted much longer and were still present at the end of the experiment. These observations were repeated three times, with similar results each time (Figure 9, see also http://public.me.com/joekoke to view the actual images as a QuickTime movie).
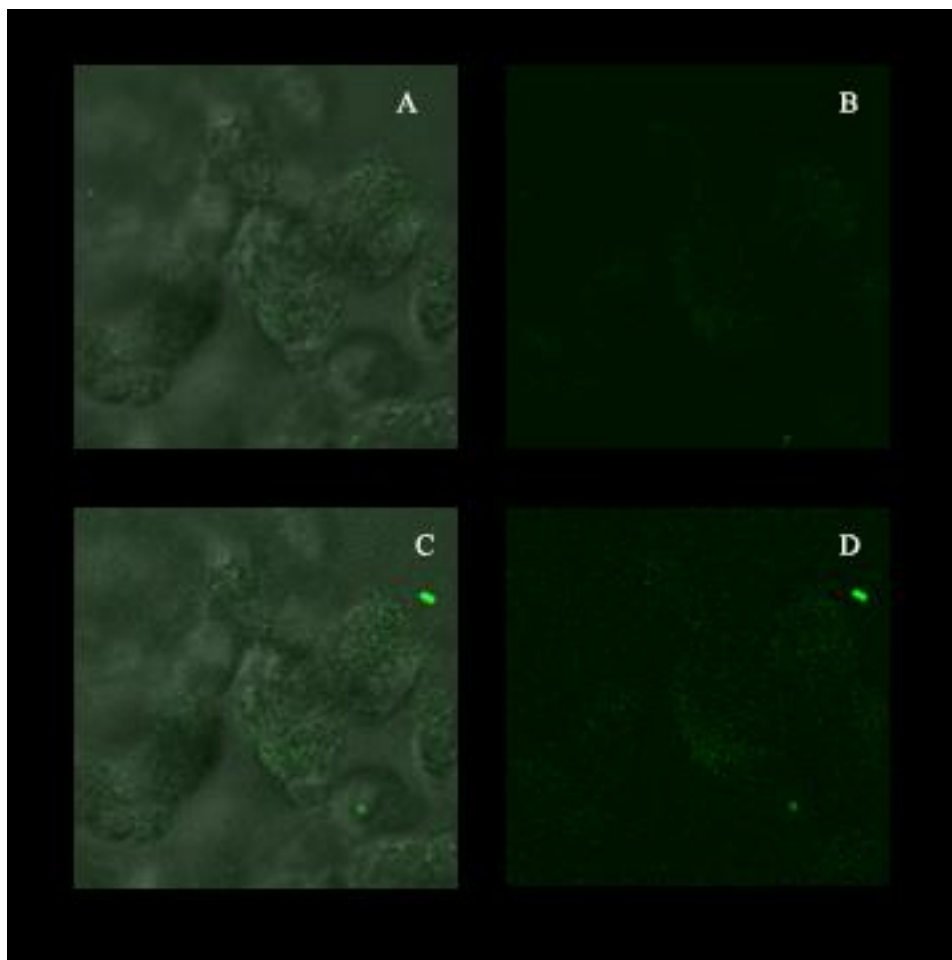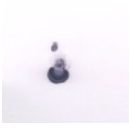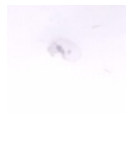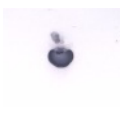
Figure 9. F98 cells loaded with Oregon Green 488 BAPTA-1 frame 1 of 250 used as a control and contains both DIC and fluorescent channels (A). F98 cells loaded with Oregon Green 488 BAPTA-1 frame 1 of 250 used as a control and contains the fluorescent channel only (B). F98 cells loaded with Oregon Green 488 BAPTA-1 frame 134 of 250 indicated increases in calcium channel activity and contains both DIC and fluorescent channels (C). F98 cells loaded with Oregon Green 488 BAPTA-1 frame 134 of 250 indicated increases in calcium channel activity and contains the fluorescent channel only (D).

D. Does mAB J1-31 recognize a phosphoepitope?

To identify if mAB J1-31 recognizes a phosphoepitope I conducted a SDS-PAGE and western analysis after the following treatments: no treatment F98 cell lysates, forskolin treated F98 cell lysates, no treatment with incubation in 48 nM of H89 for 5 minutes followed by incubation in $PP2A_1$ for 30 minutes, and forskolin treated F98 cell were extracted and then treated with H89 and $PP2A_1$ incubation as described above. Preliminary immunoblot results show that when the above 4 treatments are probed for anti-phosphoserine, both no treatment and forskolin-induced activated F98 cells lysates that have been exposed to PP2A1 show a decrease in alkaline phosphatase signal. No difference is seen when probed for lamin B, GFAP, and mAB J1-31. I would expect to see if a difference when probing for mAB J1-31 if the hypothesis that mAB J1-31 phosphorylates phospho-epitopes on both GFAP and lamin B.

Table 4. Immunoblot results to identify whether mAB J1-31 recognizes a phosphoepitope on GFAP and lamin B.

	anti-GFAP	anti-phosphoserine	mAB J1-31	anti-lamin B
No Treatment				
No Treatment + PP2A				
Forskolin				
Forskolin + PP2A				

CHAPTER IV

DISCUSSION

My results indicate that exposure of F98 cells to forskolin for as little as 7 minutes causes a significant increase in nuclear and cytoplasmic labeling of intermediate filaments by mAB J1-31. As seen in Figure 2, a significant increase in mean pixel intensity occurred within 7 minutes of forskolin incubation, reaching its peak at 30 minutes. After 30 minutes, the intensity of labeling decreases with increasing time of incubation in forskolin. Finally, at 90 minutes another peak in labeling intensity is seen with a subsequent decline in mean pixel intensity. The rapidity of the onset of forskolin activity indicates that the first peak at 30 minutes is most likely due to activation of cytoplasmic pathways (post-translational events), while the later peak at 90 minutes may result from PKA activation of CREB proteins, and activation of transcription and translation of new gene products. Dahle et al. (2005) observed that by using competitive enzyme immunoassays to measure cAMP levels in Kupffer cells, forskolin significantly elevated cAMP levels after 10 minutes or less.

In the present study, I found that pretreatment of F98 cells treatment with H89, a PKA catalytic subunit inhibitor (Chijiwa et al., (1990), abolishes the effect of forskolin and even leads to statistically significant decreases in mAB J1-31 labeling in F98 cells not treated with forskolin (Figure 7). Fetal bovine serum (FBS) contains nerve growth factor (NGF), which is known to activate adenylyl cyclase (Cremins et al., 1986). This

evidence suggests cAMP-PKA pathways are already on before the activation by

forskolin. Perhaps for this reason, F98 cells treated with H89 only show a decrease in

mAB J1-31 labeling. These differences in measured pixel intensities of reactive F98 cells

indicate that forskolin-induced activation of F98 cells occurs via a cAMP and PKA-

dependent pathway. In the neuronal cell line PC12D, forskolin-induced neurite

outgrowth was shown to be mediated through PKA as incubation in H89 prevented

neurite outgrowth (Chijiwa et al., 1990). These results suggest that cAMP activation of

PKA may not only be involved in neurite outgrowth but also in glial scar formation as

shown through this study.

F98 cells treated with forskolin only and Rp-cAMPS followed by forskolin did

not show statistically significant differences in labeling; however, they did significantly

differ from no treatment and H89, puromycin and verapamil followed by forskolin

treatments. No treatment and H89 followed by forskolin did not show significant

differences but the pair was significantly different from the other four treatments

(forskolin only, Rp-cAMPS, puromycin, and verapamil followed by forskolin). Finally,

puromycin and verapamil treatments followed by forskolin did not show significant

differences but were significantly different from the other four treatments (no treatment,

forskolin only, Rp-cAMPS and H89 followed by forskolin).

These observations indicate that it is the catalytic subunit of PKA that is active in

causing increased mAB J1-31 labeling. The catalytic subunit of PKA activates

downstream targets in many other cell signaling pathways, both nuclear via PKA

phosphorylation of CREBs (Kim et al., 2005), and cytoplasmic including cAMP-PKA

regulation of voltage-gated Ca^{+2} channels (Dai et al., 2009). Therefore, the conclusion

that inhibition of the catalytic subunit is significant in comparison to inhibition of the

regulatory subunit is plausible. Rp-cAMPS may not have shown inhibition due to

permeability; however, Gjertsen et al. (1995) showed half-maximal inhibitory

concentration of Rp-cAMPS to be between 3-20 μM. This study used a 100 μM

concentration which should have been a sufficient concentration to exclude permeability

of the inhibitor as an explanation for why Rp-cAMPS did not show inhibition.

Puromycin was not effective in modifying F98 cell response to forskolin, as

measured by mAB J1-31 labeling (Figure 7). Cytoskeletal remodeling that occurs during

reactive astrogliosis (Safavi-Abbasi et al., 2001) suggested that protein synthesis may be

necessary for the increased mAB J1-31 labeling seen in forskolin-induced activation of

F98 cells; however, this is unlikely here on the basis of puromycin's failure to prevent

increased mAB J1-31 labeling and the rapidity of the forskolin effect, as discussed above.

Interestingly, puromycin treatment of F98 cells caused increased labeling of F98 cells as

compared to untreated cells (Figure 5) and forskolin-treated cells. The reason for this is

not known, but one could speculate that the toxicity of puromycin provoked a reactive

response in the F98 cells that masked the effect of forskolin.

Verapamil, an L-type calcium channel inhibitor, was also ineffective in modifying

F98 cell response to forskolin, as measured by mAB J1-31 labeling (Figure 7). Although

inhibition of L-type calcium channels did not affect the forskolin induced increase in

mAB J1-31 labeling, other calcium channels that may be regulated directly by cAMP or

PKA cannot be ruled out. Such a pathway in forskolin-induced activation of F98 cells

may involve similar mechanisms as shown in recent studies of hydrogen sulfide (H_2S) as

a neuromodulator in neurons and glia. H_2S apparently directly activates adenlyly cyclase

in astrocytes, causing an increase in cytoplasmic Ca^{+2} that may enter through plasma membrane ion channels (Qu et al., 2008). This effect of H_2S on astrocytes suggests that cAMP-gated Ca^{2+} channels may be present on astrocytes. The activation of these channels may impact forskolin-induced activation of F98 cells and would require further investigation. Another pathway of interest may involve Ca^{2+}-dependent phosphatase or phosphodiesterases, which regulate phosphorylation and cAMP levels. Also, calcium may serve an antagonist role, which could account for increased labeling seen in panel C and D of Figure 7.

To test if forskolin treatment of F98 cells could cause Ca^{+2} transient increases in the cytoplasm, I implemented live cell imaging techniques using the calcium-sensitive fluorescent probe, Oregon Green 488 BAPTA-1. The results suggested a role for calcium channels in forskolin-induced activation of F98 cells, as an increase of calcium "sparks" was observed upon addition forskolin.

Finally to further investigate the role of J1-31 recognizing a phospho-epitope on GFAP and lamin B, I conducted immunoblots and western blot analysis of F98 cells treated with phosphatase protein PP2A. Four different treatments were tested: F98 cells treated with PP2A, F98 cells untreated, F98 cells activated by forskolin and F98 cells activated by forskolin and treated with PP2A. H89 was used to inhibit kinases. Preliminary immunoblots results, as seen in Figure 10, do not support the conjecture that mAB J1-31 is specific for a phosphoserine containing epitope. One explanation for the inconclusive results may be due to the incomplete inhibition of kinases that are phosphorylating the phospho-epitope before phosphatases can remove the phosphate

groups from the substrate. Another explanation for inconclusive results is that immunoblots are not quantitative.

Western blot results (not shown) yielded inconclusive results. When the transfer was probed using mAB J1-31 there were no bands. This is due to using antibody that is not concentrated enough to produce a result. However, previous research by García et al. (2003) has shown immunoblots of F98 cell lysates probed with mAB J1-31, polyclonal anti-GFAP, monoclonal anti-lamin B and monoclonal anti-phosphoserine. Anti-GFAP, mAB J1-31, and anti-phosphoserine recognized bands at 100 kDa. Anti-GFAP, mAB J1-31 and anti-lamin B recognized a band at 36 kDa. Finally, mAB J1-31, anti-phosphoserine, and anti-lamin B all recognized a band at 70 kDa. These results provide strong circumstantial evidence that mAB J1-31 recognizes a phosphoepitope on GFAP and lamin B and future studies should investigate this conjecture using concentrated mAB J1-31 and protein phosphatase.

Conclusions and Future Directions

The experiments presented here aimed to unfold cAMP-mediated pathways involved in astrocytes transitioning from a quiescent state to a reactive state. Based on these results and results of others preceding me, I conclude that forskolin-induced activation of F98 cells proceeds through activation of adenlyly cyclase, increased production of cAMP which then activates the catalytic subunits of PKA, which then leads to increased labeling by mAB J1-31. Does PKA directly phosphorylate IFs, or is the intracellular signaling pathway in astrocytes transitioning from a quiescent state to a reactive state dependent upon calcium channels? In the scope of this project, this question will remain largely unanswered. It is evident that L-type calcium channels are

not involved in increasing J1-31 immunoreactivity; however, the presence of other types of calcium channels may need to be further explored to investigate the role of calcium channels in reactive astrogliosis. MALDI-MS should be used to further characterize mAB J1-31 and the phospho-epitopes that the antibody recognizes.

REFERENCES

Agrawal, S.K., Nashmi, R., and Fehlings, M.G. (2000). Role of L- and N-type calcium channels in the pathophysiology of traumatic spinal cord white matter injury. *Neuroscience* **99**(1): 179-188.

Agulhon, C., Petravicz, J., McMullen, A.B., Sweger, E.J., Minton, S.K., Taves, S.R., Casper, K.B., Fiacco, T.A. and McCarthy, K.D. (2008). What is the role of astrocyte calcium in neurophysiology? *Neuron* **59**: 932-946.

Berridge, M.J., Bootman, M.D., and Roderick, H.L. (2003). Calcium signalling: dynamics, homeostasis and remodelling. *Nature Reviews Molecular Cell Biology* **4**: 517-529.

Braet, K., Cabooter, L., Paemeleire, K. and Leybaert, L. (2004). Calcium signal communication in the central nervous system. *Biol Cell* **96**: 79-91.

Cai, D., Shen, Y., De Bellard, M., Tang, S., and Filbin, M.T. (1999). Prior exposure to neurotrophins blocks inhibition of axonal regeneration by MAG and myelin via a cAMP-dependent mechanism. *Neuron* **22**: 89-101.

Chen, Y. and Swanson, R.A. (2003). Astrocytes and brain injury. *Journal of Cerebral Blood Flow & Metabolism* **23**: 137-149.

Chijiwa, T., Mishima, A., Hagiwara, M., Sano, M., Hayashi, K., Inoue, T., Naito, K., Toshioka, T. and Hidaka, H. (1990). Inhibition of forskolin-induced neurite outgrowth and protein phosphorylation by a newly synthesized selective inhibitor of cyclic AMP-dependent protein kinase, N-{2-(p-bromocinnamylamino)ethyl}-5-isoquinolinesulfonamide (H-89), of PC12D Pheochromocytoma cells **265** (9): 5267-5272.

Choi, B.H. and Kim, R.C. (1984). Expression of glial fibrillary acidic protein in immature oligodendroglia. *Science* **223**: 407-408.

Correa-Cerro, L.S. and Mandell, J.W. (2007). Molecular mechanisms of astrogliosis: new approaches with mouse genetics. *J Neuropathol Exp Neurol* **66**: 169-176.

Cremins, J., Wagner, J.A. and Halegoua, S. (1986). Nerve growth factor action is mediated by cyclic AMP and Ca2+/Phospholipid-dependent protein kinases. The Journal of Cell Biology 103: 887-893.

Dahl, D., Miles, N.H., Nguyen, B.T. and Bignami, A. (1982). Glial fibrillary acidic (GFA) protein in Schwann cells: fact or artifact? *J Histochem Cytochem* **30**: 912-918.

Dahle, M.K., Myhre, A.E., Aasen, A.O. and Wang, J.E. (2005). Effects of forskolin on Kupffer cell production of interleukin-10 and tumor necrosis factor alpha differ from those of endogenous adenylyl cyclase activators: possible role for adenylyl cyclase 9. *Infection and Immunity* **73**(11): 7290-7296.

Dai, S., Hall, D.D. and Hell, J.W. (2009). Supramolecular assemblies and localized regulation of voltage-gated ion channels. *Physiol Rev* **89**: 411-452.

Eng, L.F. and Ghirnikar, R.S. (1994). GFAP and astrogliosis. *Brain Pathology* **4**: 229-237.

García, D.M. and Koke, J.R. (2009). Astrocytes as gate-keepers in optic nerve regeneration-A mini-review. *Comparative Biochemistry and Physiology* **152**: 135-138.

García, D.M., Weigum, S.E., and Koke, J.R. (2003). GFAP and nuclear lamins share an epitope recognized by monoclonal antibody J1-31. *Brain Research* **976**: 9-21.

Gjertsen, B.T., Mellgren, G., Otten, A., Maronde, E., Genieser, H.G., Jastorff, B., Vintermyr, O.K., McKnight, G.S., and Stein, O.D. (1995). Novel (Rp)-cAMPS analogs as tools for inhibition of cAMP-kinase in cell culture. *The Journal of Biological Chemistr*y **270**(35): 20599-20607.

Hatfield, J.S., Skoff, R.P., Maisel, H. and Eng, L. (1984). Glial fibrillary acidic protein is localized in the len epithelium. *The Journal of Cell Biology* **98**: 1895-1898.

Herrmann, J.E., Imura, T., Song, B., Qi, J., Ao, Y., Nguyen, T.K., Korsak, R.A., Takeda, K., Akira, S. and Sofroniew, M.V. (2008). STAT3 is a critical regulator of astrogliosis and scar formation after spinal cord injury. *J Neurosci* **28**(28): 7231-7243.

Iwami, G., Kawabe, J., Ebina, T., Cannon, P.J., Homey, C.J. and Ishikawa, Y. (1995). Regulation of adenylyl cyclase by protein kinase a. *The Journal of Biological Chemistry* **270**(21): 12481-12484.

Kamenetsky, M., Middelhaufe, S., Bank, E.M., Levin, L.R., Buck, J. and Steegborn, C. (2006). Molecular details of cAMP generation in mammalian cells: a tale of two systems. *Journal of Molecular Biology* **362**: 623-639.

Kim, C., Xuong, N. and Taylor, S. (2005). Crystal structure of a complex between the catalytic and regulator (RIalpha) subunits of PKA. *Science* **307**: 690-696.

Kohyama, J., Kojima, T., Takatsuka, E., Yamashita, T., Namiki, J., Hsieh, J., Gage, F.H., Namihira, M., Okano, H., Sawamoto, K. and Nakashima, K. (2008). Epigenetic regulation of neural cell differentiation plasticity in the adult mammaliam brain. *Proc Natl Acad Sci* **105**: 18012-18017.

Makino, N., Mise, T., and Sagara, J. (2008). Kinetics of hydrogen peroxide elimination by astrocytes and C6 glioma cells analysis based on a mathematical model. *Biochem Biophys Acta* **1780**: 927-936.

Malhotra, S.K., Luong, L.T., Bhatnagar, R. and Shnitka, T.K. (1997). Up-regulation of reactive astrogliosis in the rat glioma 9L cell line by combined mechanical and chemical injuries. *Cytobios* **89**: 115-134.

Malhotra, S.K., Bhatnagar, R., Shnitka, T.K., Herrera, J.J., Koke, J.R. and Singh, V. (1995). Rat glioma cell line as a model for astrogliosis. *Cytobios* **82**: 39-51.

Malhotra, S.K., Shnitka, T.K., and Elbrink, J. (1990). Reactive astrocytes--a review. *Cytobios* **61**: 133-160.

Malhotra, S.K., Predy, R., Johnson, E.S., Singh, R. and Leeuw, K. (1989). Novel astrocytic protein in multiple sclerosis plaques. *Journal of Neuroscience Research* **22**: 36-49.

Malhotra, S.K., Wong, F., Cumming, P., Ross, S.D., Shnitka, T.K., Manickavel, V., Warren, K.G. and Jeffrey, V. (1984). A monoclonal antibody for cytoskeletal antigenic determinant(s) distinguishable from glial fibrillary acidic protein in astrocytes. *Microbios Letters* **26**: 151-157.

Morga, E., Mouad-Amazzal, L., Felten, P., Heurtaux, T., Moro, M., Michelucci, A., Gabel, S., Grandbarbe, L. and Heuschling, P. (2009). Jagged 1 regulates the activation of astrocytes via modulation of NFkappaB and JAK/STAT/SOCS pathways. *Glia* **57**(16): 1741-1753.

Nagai, Y., Tsugane, M., Oka, J. and Kimura, H. (2004). Hydrogen sulfide induces calcium waves in astrocytes. *FASEB J* **18**: 557-559.

Nathans, D. (1964). Puromycin inhibition of protein synthesis: incorporation of puromycin into peptide chains. *PNAS* **51**: 585-592.

Obrig, T.G., Culp, W.J., McKeehan, W.L. and Hardesty, B. (1970). The mechanism by which cycloheximide and related glutarimide antibiotics inhibit peptide synthesis on reticulocyte ribosomes. *The Journal of Biological Chemistry* **246**(1):174-181.

Pekny, M. and Nilsson, M. (2005). Astrocyte Activation and Reactive Gliosis. *Glia* **50**: 427-434.

Pekny, M. and Pekna, M. (2004). Astrocyte intermediate filaments in CNS pathologies and regeneration. *Journal of Pathology* **204**: 428-437.

Preddy, R., Malhotra, S.K., and Das, G.D. (1988). Enhanced expression of a protein antigen (J1-31 antigen, 30 kilodaltons) by reactive astrocytes in lacerated spinal cord. *Journal of Neuroscience Research* **19**: 397-404.

Preddy, R., Singh, D., Bhatnagar, R. Singh, R., and Malhotra, S.K. (1987). A new protein (J1-31 antigen, 30kD) is expressed by astrocytes, Müller glia, and ependyma. *Bioscience Reports* **7**(6): 491-502.

Ramsey, G. 2005. Phosphorylation of GFAP and lamin B and astrocyte activation as revealed by monoclonal antibody J1-31, Thesis, Texas State University.

Qu, K., Lee, S.W., Bian, J.S., Low, C.M. and Wong, P.T. (2008). Hydrogen sulfide: neurochemistry and neurobiology. *Neurochem Int* **52**: 155-165.

Qui, J., Cai, D., Dai, H., McAtee, M., Hoffman, P.N., Bregman, B.S., and Filbin, M.T. (2002). Spinal axon regeneration induced by elevation of cyclic AMP. *Neuron* **34**: 895-903.

Schemes, E. and Giaume, C. (2006). Astrocyte calcium waves: what they are and what they do. *Glia* **54**(7): 716-725.

Schroder, H. and Malhotra, S.K. (1987). Characterization of rodent pineal astrocytes by immunofluorescence microscopy using a monoclonal antibody (J1-31). *Cell Tissue Res* **248**: 607-610.

Seamon, K.B., Padgett, W. and Daly, J.W. (1981). Forskolin: unique diterpene activator of adenylate cyclase in membranes and in intact cells. *Proc Natl Acad Sci* 7**8**(6): 3363-3367.

Serezani, C.H., Ballinger, M.N., Aronoff, D.M. and Peters-Golden, M. (2008). *American Journal of Respiratory Cell and Molecular Biology* **39**: 127-132.

Silver, J. and Miller, J.H. (2004). Regeneration beyond the glial scar. Nature Reviews Neuroscience **5**: 146-156.

Singh, R., Singh, B., and Malhotra, S.K. (1986). A new "marker" protein for astrocytes. *Bioscience Reports* **6**(1): 73-79.

Singh, M., Price, K., Bhatnagar, R., Johnson, E., and Malhotra, S. (1992). J1-31 antigen of astrocytes: cytoplasmica and nuclear localization. *Dendron* **1**: 91-108.

Sriram, K., Benkovic, S.A., Hebert, M.A., Miller, D.B. and O'Callaghan, J.P. (2004). Induction of gp130-related cytokines and activation of JAK2/STAT3 pathway in

astrocytes precedes up-regulation of glial fibrillary acidic protein in the 1-methyl-4-phenyl-1,2,3,6-tetrahydropyridine model of neurodegeneration. *Journal of Biological Chemistry* **279**(19): 19936-19947.

Stevenson, P. 1996. Biochemical characterization of a possible precursor to glial fibrillary acidic protein in reactive astrocytes, Thesis, Texas State University.

Studzinski, G.P. and Love, R. (1964). Effects of puromycin on the nucleoproteins of the hela cell. *The Journal of Cell Biology* **22**: 493-503.

Svendsen, C.N. (2002). The amazing astrocyte. *Nature* **417**: 29-32.

Temburni, M.K. and Jacob, M.H. (2001). New functions for glia in the brain. *PNAS* **98**(7): 3631-3632.

Wang, E., Cairncross, J.G. and Liem, K.H. (1984). Identification of glial filament protein and vimentin in the same intermediate filament system in human glioma cells. *Proc. Natl. Acad. Sci.* **81**: 2102-2106.

Watt, F.M. (1984). Selective migration of terminally differentiating cells from the basal layer of cultured human epidermis. *The Journal of Cell Biology* **98**: 16-21.

Won, C. and Oh, Y.S. (2000). cAMP-induced stellation in primary astrocyte cultures with regional heterogeneity. Brain Research **887**(2): 250-258.

Yang, H., Cheng, X.P., Li, J.W., Yao, Q. and Ju, G. (2009). De-differentiation response of cultured astrocytes to injury induced by scratch or conditioned culture medium of scratch-insulted astrocytes. *Cell Mol Neurobiol* **29**(4): 455-473.

Yen, S.H. and Fields, K.L. (1981). Antibodies to neurofilament, glial filament, and fibroblast intermediate filament proteins bind to different cell types of the nervous system. *J Cell Biol* **88**:115-126.

VITA

Mayuri Pankaj Patel (Mya) was born to Pankaj and Bharati Patel in 1984. She was raised in Paris, Texas, graduating from North Lamar High School. Mya attended Baylor University as a Biology major in 2002. She graduated from Baylor University in 2006 with a B.A. in Biology and a minor in Chemistry. In 2007, she attended Texas State University-San Marcos to pursue a Masters of Science degree in Biology. While at Texas State, she worked as an instructional assistant for Anatomy and Physiology and Cellular Physiology. She served as Vice President for the Pre-Optometry Professional Soceity from 2007-2008, Secretary for Tri Beta from 2008-2009, and Treasurer for the Biology Graduate Student Organization from 2008-2009. She hopes to attend Baylor College of Medicine and enter the Physician's Assistant Program.

Permanent Address: 3055 Oak Creek Dr.

Paris, TX 75462

This thesis was typed by Mayuri Pankaj Patel.